Observation of a metamagnetic phase transition in an itinerant $4f$ system via the magneto-optic Kerr effect: $Ce(Fe_{1-x}Co_x)_2$

R. J. Lange, I. R. Fisher, P. C. Canfield, V. P. Antropov, S. J. Lee, B. N. Harmon, and D. W. Lynch
Ames Laboratory and Department of Physics and Astronomy, Iowa State University, Ames, Iowa 50011
(Received 1 July 1999; revised manuscript received 26 May 2000)

The optical and magneto-optical properties of single crystals of YFe_2, $CeFe_2$, and $Ce(Fe_{1-x}Co_x)_2$ ($x \simeq 0.1$) were measured between 1.4 and 5.0 eV using a rotating-analyzer ellipsometer and a normal-incidence polar Kerr spectrometer. The electronic structures and optical properties of YFe_2 and $CeFe_2$ were calculated using the tight-binding linear muffin-tin orbital method in the atomic-sphere approximation. For YFe_2 the calculations reproduce the experimental spectra. Alloying $CeFe_2$ with small amounts of Co leads to an electronic instability which is evidenced by a low-temperature antiferromagnetic (AF) phase. The Kerr effect was measured in the AF and field-induced ferromagnetic (FM) regime. A remarkably large Kerr rotation was measured even in the AF state (up to $-1°$). The phase transition from AF to FM order was observed in the Kerr rotation spectra at 5 and 50 K at photon energies of 1.8 and 4.0 eV.

I. INTRODUCTION

The nature of the anomalous magnetic properties of $CeFe_2$ has been of great interest for the last two decades. RFe_2 compounds with heavy rare earths have a high ordering temperature, a large magnetocrystalline anisotropy, and a reasonably strong magneto-optic signal, which makes those materials suitable for magneto-optic device applications.[1,2] $CeFe_2$ clearly is an exception, having an ordering temperature that is reduced to below room temperature. This already suggests some unusual interactions which are manifested in a low-temperature antiferromagnetic structure upon alloying with small amounts of Al, Co, or Ru.[3–6] The lattice constant of $CeFe_2$ is smaller than expected for a rare-earth-Fe_2 compound containing a trivalent Ce ion.[7] X-ray photoemission spectroscopy (XPS) indicates that, in fact, the Ce ion is close to the tetravalent state in $CeFe_2$.[8] Neutron scattering experiments indicated a magnetic moment of $-0.14\mu_B$/Ce which originates from $4f$ and $5d$ contributions.[9] It is believed that $CeFe_2$ is an itinerant magnet, similar to UFe_2,[10,11] and that the $4f$ overlap is strong enough to broaden the usually localized $4f$ states into bands. Recently, rather strong antiferromagnetic fluctuations were unexpectedly found in the ferromagnetically ordered state of $CeFe_2$.[7] We performed magneto-optic measurements on $CeFe_2$ to gain more insight into the electronic structure of this intriguing compound. In order to be able to separate out contributions from the $4f$ states the same experiments were performed on the Y analog which has no $4f$ electrons but behaves chemically similar to RFe_2. We then investigated a $Ce(Fe_{1-x}Co_x)_2$ alloy to learn more about the character of the metamagnetic phase transition and how it relates to the magneto-optical signal.

II. SAMPLE PREPARATION

R-Fe_2 compounds were grown by the self-flux-growth technique from a rare-earth rich melt.[12,13] The crystals were grown from Ames Lab 99.995% Ce, Ames Lab 99.99% Y, and 99.999% Fe and Co from Union Carbide. The flux growth yielded platelike crystals, with the plane of the plates perpendicular to [111]. The YFe_2 and $CeFe_2$ crystals were about $3\times5\times2\,mm^3$ and had clean surfaces. No further surface treatment was necessary and the as-grown crystals were used for the optical experiments. A $Ce(Fe_{1-x}Co_x)_2$ alloy was grown from a pseudobinary melt. A nominal $x=0.2$ resulted in an estimated $x\simeq0.1$ (see Sec. III). This growth produced crystals of octahedral morphology about $3\times3\times3\,mm^3$ in size with clean triangular (111) facets. As for the other samples of this group, polishing was not necessary. However, RFe_2 compounds are rather reactive and complete oxidation of a sample surface can occur in as little as one hour, giving the surface a yellowish, instead of the typical metallic, appearance of an unoxidized surface. Lee encountered this problem when measuring heavy rare-earth-Fe_2 compounds.[14] In many cases samples needed to be polished, which led to thick oxide overlayers which reduced the magnitude of the optical conductivity. After the samples were removed from the growth crucible and separated from the flux they were immediately sealed in pyrex ampules with a partial pressure of argon. Samples were kept sealed until the optical experiments were performed. Immediately before the experiments the glass was broken, the sample epoxied to the sample holder, and transferred into the sample chamber where it was kept in a He atmosphere during the measurements. The sample was in contact with air for no longer than a total of 10 min. Paolasini *et al.*[7] performed neutron scattering on similar samples grown at Ames Lab and pointed out that $CeFe_2$ is extremely sensitive to thermal shock. In one hour they transformed one 5-gm single crystal into powder by warming it from low temperature to room temperature. Slow cooling and heating is therefore necessary with $CeFe_2$ and the Ce-Fe-Co alloy discussed in this paper. After the magneto-optical experiment, the dielectric function was measured on the same samples. Since ellipsometry cannot be performed in vacuum or an inert atmosphere using our experimental setup, the samples were exposed to air for up to 30 min during the measurement. Before each scan the surface was polished with 0.05 μm alumina to remove any ox-

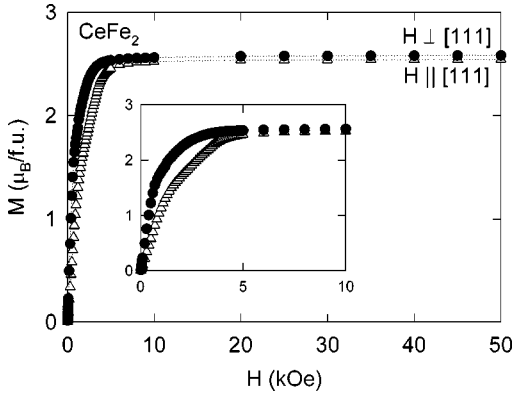

FIG. 1. M/H (upper panel) and χ^{-1} (lower panel) as a function of temperature for $CeFe_2$ at 1 kOe. Data shown in the lower panel were taken with $H\|[111]$.

ide that might have formed on the surface. Ellipsometric spectra were precise to within 2%, which is considered the accuracy of our instrument. However, oxidation of the top layer occurs on a much shorter time scale (on the order of ns for Al) and there will always be a native oxide overlayer if the measurements cannot be performed under UHV conditions.

$R Fe_2$ compounds crystallize in the cubic $MgCu_2$ Laves phase structure ($C15$, space group O_h^7, $Fd\bar{3}m$). The lattice constants for YFe_2 (Ref. 15) and $CeFe_2$ (Ref. 7) are 7.363 and 7.304 Å, respectively. These values were also used for the band structure (BS) calculations. The lattice constant of $CeFe_2$ is much smaller (similar to that of $HoFe_2$) than expected for a compound containing tripositive Ce, indicating valence fluctuations.[8,16]

III. MAGNETIZATION

In order to characterize the samples, dc magnetization measurements were made on all specimens, using a commercial Quantum Design SQUID magnetometer. YFe_2 is a ferromagnet with an ordering temperature of 528 K.[17] At 55 kOe, the limit of our instrument, a saturated moment of $2.91\mu_B/YFe_2$ was measured at 5 K, the same value obtained by Buschow and van Stapele at 4.2 K.[15] Polarized neutron studies by Ritter *et al.*[18] revealed an Y moment as large as $-0.67\mu_B$ coupled ferrimagnetically to an Fe moment of $1.77\mu_B$. The total saturated moment agrees with our magnetization data. The easy direction of magnetization is along [111], i.e., along the surface normal of the (111) facets.[1]

$M(T)$ for $CeFe_2$ in an external field of 1 kOe is shown in Fig. 1. The upper panel shows M/H between 100 and 350 K, and emphasizes the anisotropic behavior that is also found in $M(H)$. In the lower panel $\chi^{-1}(T)$ is plotted which allows one to determine roughly the ordering temperature. A fit of $\chi^{-1}(T)$ above 280 K gives $T_C \approx 240$ K. A proper determination of T_C requires detailed $M(H)$ data for temperatures above and below the ordering temperature. Following the method of Arrott,[19] plots of M^3 versus field between 220 and 250 K with the field applied parallel to [111] lead to an estimate of $T_C = (228 \pm 2)$ K, in excellent agreement with the 230 K measured by Farrell and Wallace.[20] From a fit of χ^{-1} above 280 K an effective moment of $4.87\mu_B$ was derived.

At 10 K the easy axis is perpendicular to [111], i.e., in the surface plane. The anisotropy is small and the saturated moments for $H\|[111]$ and $H\perp[111]$ differ by less than 2%. The moment reached at 55 kOe for $H\|[111]$ is $2.55\mu_B/CeFe_2$. This is the same alignment used in the optical experiments. The high-temperature susceptibility indicates a Curie constant too large to be attributed solely to the Fe ions. There is a contribution from Ce, observed in later experimental studies employing polarized neutrons,[9] x-ray magnetic circular dichroism (XMCD),[21–23] Compton scattering,[24] and nuclear magnetic resonance (NMR).[25] Kennedy *et al.*[5,26] noticed reflections of antiferromagnetic origin but did not investigate this further. An antiferromagnetic component of $0.15\mu_B$/Ce was estimated. Upon doping with Al, Co, or Ru they found an antiferromagnetic ground state with wave vector $[\frac{1}{2},\frac{1}{2},\frac{1}{2}]$. In the case of $Ce(Fe_{0.8}Co_{0.2})_2$ a lattice distortion from cubic ($\alpha = 90°$) to rhombohedral symmetry with $\alpha = 90.2°$ was found.[26,27] The most recent results from neutron inelastic scattering on $CeFe_2$ confirmed antiferromagnetic fluctuations in the ferromagnetically ordered state.[7] It is concluded that in $CeFe_2$ there is a strong competition between the ferromagnetic ground state and an antiferromagnetic state with the same wave vector that was found earlier by Kennedy *et al.*[5,26] The apparent static antiferromagnetic component is about $0.05\mu_B$, superimposed on a $1.2\mu_B$ ferromagnetic Fe moment. At low temperatures these antiferromagnetic correlations extend over many unit cells. It is therefore likely that $CeFe_2$ is close to an electronic instability and a small change in electron concentration can establish a stable antiferromagnetic ground state.

Alloying reduces T_C and, as mentioned above, a low-temperature simple antiferromagnetic phase is found upon substitution for Fe by Co, Al, Ru, Rh, or Pd.[3–6] In $Ce(Fe_{1-x}Co_x)_2$ a low-temperature antiferromagnetic phase is found for $0 < x < 0.3$. For $0.3 < x < 1$ ferromagnetic order persists down to low temperatures. The paramagnetic-to-ferromagnetic and ferromagnetic-to-antiferromagnetic phase transitions were observed in neutron scattering,[5,26,27] susceptibility,[3,4] resistivity and thermopower,[6] specific heat,[28–30] and thermal expansion experiments.[27,31] An abrupt change in the cell volume at the ferromagnetic to antiferromagnetic transition indicates that this is a first-order phase transition. The phase transition from the paramagnetic to ferromagnetic regime is accompanied by a smooth variation in cell volume and is therefore believed to be of second order.

Figure 2 shows magnetization versus temperature for the Ce(Fe/Co) pseudobinary sample between 0 and 300 K in a 1 kOe applied field. We can identify two magnetic phase transitions. A plot of $d(\chi T)/dT$ (lower panel) gives a T_C of approximately 191 K, indicating the paramagnetic to ferromagnetic transition. A linear fit to the high temperature $\chi^{-1}(T)$ data yields an effective moment of $4.97\mu_B$, slightly larger than that obtained for $CeFe_2$, and 207 K for Θ. At lower temperature there is a second phase transition from the ferromagnetic to an antiferromagnetic structure at $T_N = 81$ K. In the upper panel of that figure we indicate the regimes of antiferromagnetic (AFM) and ferromagnetic (FM) order. Above T_C the sample behaves paramagnetically (PM). Using the values obtained for T_C and T_N and the phase diagram for $Ce(Fe_{1-x}Co_x)_2$ (Refs. 27–29,31,32) we estimate $8.5\% < x$

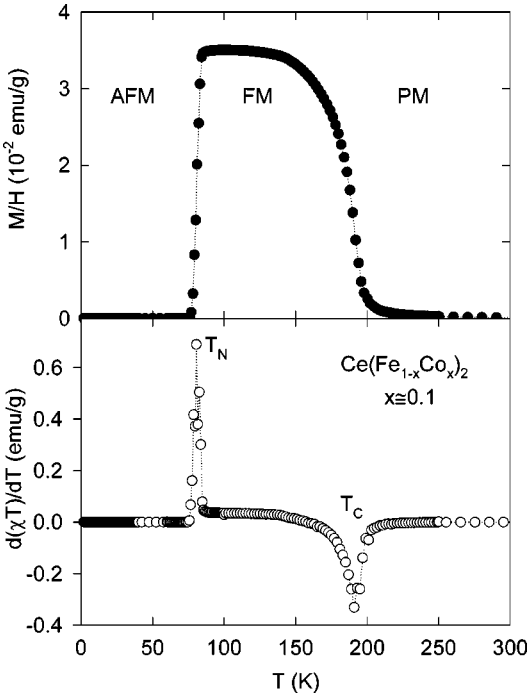

FIG. 2. Temperature-dependent magnetization of $Ce(Fe_{1-x}Co_x)_2$ with a field of 1 kOe applied perpendicular to [111]. The upper panel shows M/H, indicating two phase transitions. The antiferromagnetic (AFM), ferromagnetic (FM), and paramagnetic (PM) regimes are indicated in the figure. From $d(\chi T)/dT$, which is shown in the lower panel, we estimate $T_N \simeq 81$ K and $T_C \simeq 191$ K.

$<10\%$. We obtain a range for x since the magnetization was measured in an applied field and it is well known that T_N is field dependent.[31,32] For an unambiguous determination of T_N we would need to measure the zero-field magnetization. However, for our purposes the exact composition is not crucial and we will assume that $x \simeq 0.1$.

As in pure $CeFe_2$ the easy direction of magnetization in $Ce(Fe_{0.9}Co_{0.1})_2$ is in the plane, perpendicular to [111]. For $H \| [111]$ (Fig. 3) a saturated moment of $2.20\mu_B$/$Ce(Fe_{0.9}Co_{0.1})_2$ was measured at 50 K. If the field is applied perpendicular to [111], a maximum moment of $2.33\mu_B$ is reached. In Fig. 3 we show the magnetization versus field for

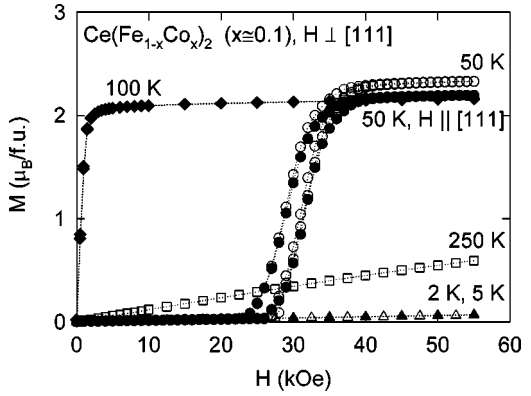

FIG. 3. $M(H)$ for $Ce(Fe_{1-x}Co_x)_2 (x \simeq 0.1)$ with $H \perp [111]$. Temperatures are indicated in the figure. At 50 K data for $H \| [111]$ are also included.

various temperatures and $H \perp [111]$. At low temperatures the sample is in a stable antiferromagnetic regime and even a field of 55 kOe is not sufficient to induce ferromagnetic ordering. At the highest field the total moment at 2 and 5 K is below $0.1\mu_B$. A field of about 68 kOe will eventually induce a ferromagnetically ordered state at this temperature,[29] also found in our spectroscopic data (see below). At 50 K the structure becomes unstable at a lower field and we observe a metamagnetic transition between 25 and 30 kOe leading to a field-induced ferromagnetic structure. Below the transition temperature the moment remains less than $0.05\mu_B$, saturating around 50 kOe at 50 K, close to the transition. We note some hysteresis which increases with decreasing temperature, consistent with the previously mentioned first-order phase transition.[29] Based on neutron experiments,[7] which showed the coexistence of ferromagnetic and antiferromagnetic spin waves, even in the parent compound, we believe that the hysteresis in $M(H)$ is caused by the competition of a ferromagnetic and antiferromagnetic ground state. At 100 K we find simple ferromagnetic order (compare Fig. 2) and saturation is reached at 5 kOe (as the domains align in the applied field). Compared to the data at 50 K, the moment is reduced which is due to thermal disorder. The scan at 250 K indicates a linear field dependence of the magnetization as expected for a paramagnet.

IV. ELECTRONIC STRUCTURE

Over the past decade rare-earth compounds have been the subject of many LDA studies due to their intriguing electronic and magnetic properties. For an excellent review on this topic we refer to an article by Brooks and Johansson.[11]

To aid in interpreting our spectra we carried out *ab initio* band structure calculations for YFe_2 and $CeFe_2$, using the local-density approximation (LDA) and the tight-binding linear muffin-tin orbital method in the atomic-sphere approximation,[33] adding spin-orbit coupling in every iteration to self-consistency. The local spin-density approximation was used for the exchange and correlation potential with the von Barth-Hedin parametrization.[34] Details are given elsewhere.[62] The interband optical conductivity tensors were calculated using Kubo's linear response theory.[35]

We do not show the band structures and total densities of states, for they resemble those published.[11,36–41] The LDA may not be so bad for the $4f$ states in $CeFe_2$, for these states form a reasonably broad band; our calculated width is 1.5 eV. Eriksson *et al.*[38] correctly predicted with the LDA the Ce and Fe moments and the ferrimagnetic alignment before they were known experimentally.

V. OPTICAL AND MAGNETO-OPTICAL RESPONSE

In general, the dielectric response of a cubic crystal magnetized along z is described by the optical conductivity tensor

$$\vec{\sigma} = \begin{pmatrix} \sigma_{xx} & \sigma_{xy} & 0 \\ -\sigma_{xy} & \sigma_{xx} & 0 \\ 0 & 0 & \sigma_{zz} \end{pmatrix}. \quad (1)$$

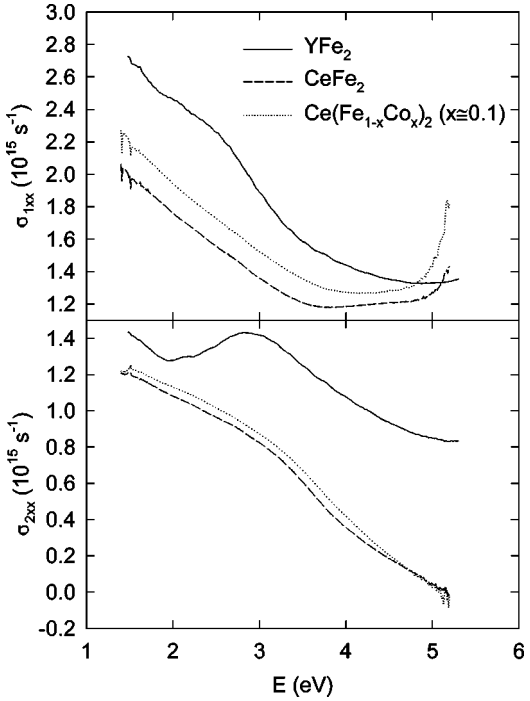

FIG. 4. Diagonal part of the optical conductivity for YFe_2, $CeFe_2$, and $Ce(Fe_{1-x}Co_x)_2$ ($x \simeq 0.1$) measured at room temperature. The upper (lower) panel shows the absorptive (dispersive) part of σ_{xx}.

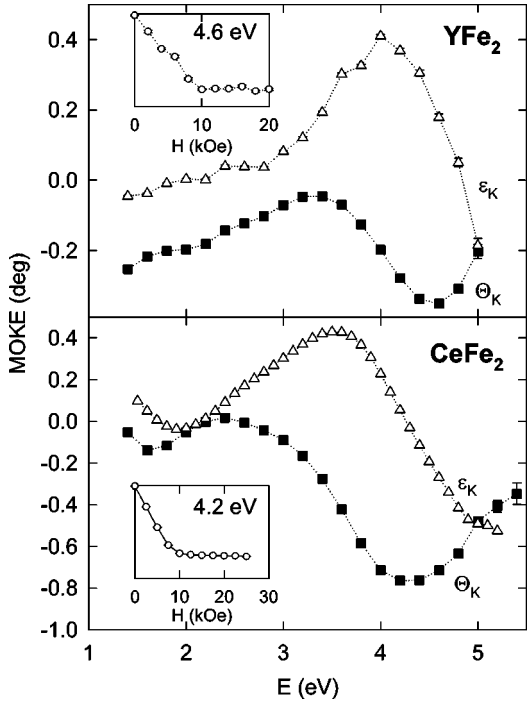

FIG. 5. Kerr rotation (Θ_K) and ellipticity (ϵ_K). Upper panel: YFe_2 at 3.5 K and 15 kOe. Lower panel $CeFe_2$ at 10 K and 10 kOe. The insets show the field dependence of Θ_K at the energy of maximum Kerr rotation.

In a nonmagnetic isotropic sample this reduces to the complex optical conductivity $\sigma_{xx}=\sigma_{1xx}+i\sigma_{2xx}=\sigma_{zz}$ and $\sigma_{xy}=0$. The diagonal elements of the optical conductivity σ_{xx} were measured at room temperature in zero magnetic field using a rotating analyzer ellipsometer (RAE).[43–45] All ellipsometric measurements were made at room temperature with no magnetic field applied. σ_{xy} was derived from σ_{xx} and the magneto-optic polar Kerr effect (MOKE), which was measured near normal incidence ($\phi<4°$). Incoming, linearly polarized light will be elliptically polarized after reflection with an ellipticity ϵ_K and the major axis of the ellipse will be rotated by an angle Θ_K. For small angles in the polar geometry the MOKE can be expressed in terms of the complex optical conductivity[46,47]

$$\Theta_K + i\epsilon_K = -\frac{\sigma_{xy}}{\sigma_{xx}}\left(1+i\frac{\sigma_{xx}}{\epsilon_0\omega}\right)^{-1/2}. \qquad (2)$$

The MOKE was measured using a polarization modulation technique employing a photoelastic modulator.[48–55] The samples were mounted in an optical cryostat with a split-coil superconducting magnet system. Data can be taken at temperatures ranging from 2 to 300 K and magnetic fields of up to 70 kOe.

We measured the dielectric function of YFe_2, $CeFe_2$, and $Ce(Fe_{1-x}Co_x)_2$ ($x \simeq 0.1$). As mentioned earlier the samples were exposed to air during the measurements. Before each scan the sample surface was lightly polished with 0.05 μm alumina abrasive to remove the oxide overlayer. Figure 4 shows the diagonal part of the optical conductivity. The absorptive part (upper panel) of YFe_2 is similar to that of the other rare-earth-Fe_2 compounds measured by Lee[14] and agrees well with the conductivity measured by Sharipov *et al.*[56] σ_{1xx} decreases monotonically, showing a weak shoulder around 2.7 eV. This feature is more pronounced in σ_{2xx}. The two compounds containing Ce are very similar. The small difference in magnitude ($<10\%$) is likely to be caused by oxidation effects. We also notice an increase of σ_{1xx} above 5 eV, ascribed to small light intensity. The absorption peak found in YFe_2 is washed out in these two compounds. However, analyzing σ_{2xx} we recognize a shoulder at 3 eV which coincides with the maximum found for YFe_2. It seems justified to say that we observe the same basic structure in all three compounds with a decrease of the absorption at 2 eV for $CeFe_2$ and $Ce(Fe_{0.9}Co_{0.1})_2$. Rhee found transitions occurring around the Γ point to give the main contribution to the 2.5 eV shoulder in YFe_2 and $LuFe_2$. There is a region in the band structure around Γ where the bands disperse very little, leading to a large DOS. The bands around 0.5 to 1 eV below E_F are of Fe-(p,d) and Y-(p,d) character. Flat bands are also found about 2 eV above E_F. The bands in that range are of Fe-d as well as Y-d character, mixed with equal amounts of Y-derived (s,p) states. Transitions involving p-derived states give large contributions to the optical conductivity and we agree with the assignment suggested by Rhee that the prominent feature in σ_{1xx} originates from transitions around the center of the BZ.

Figure 5 shows the Kerr rotation and ellipticity for YFe_2 and $CeFe_2$. YFe_2 was measured at 3.5 K in 15 kOe. From the inset we see that the Kerr rotation saturates at 10 kOe, significantly higher than the magnetization saturation of only 2 kOe at 5 K. The magnitude of the Kerr effect is rather small, reaching a minimum rotation of nearly $-0.3°$ at 4.6 eV. The ellipticity shows a maximum of 0.42° at 4 eV. The overall shape of the spectrum closely resembles that of the heavier RFe_2 compounds.[14,2] The lower panel shows data for

TABLE I. Maximum Kerr rotation $\Theta_{K,\max}$ reached at energy $E_{\max}$. Temperature T and field H at which the data were taken are given together with the sample magnetization M under those conditions. The last column gives the specific Kerr rotation per Bohr magneton.

	$E_{\max}$ (eV)	$\Theta_{K,\max}$ (°)	T (K)	H (kOe)	M (μ_B/f.u.)	$\Theta_{K,\max}/M$ (°/μ_B)
YFe_2	4.6	−0.35	3.5	15	2.91	−0.12
$CeFe_2$	4.2	−0.76	10	10	2.58	−0.29
$GdFe_2$[a]	3.8	−0.28	7	14	3.50	−0.08
$TbFe_2$[a]	4.6	−0.48	295	5	2.00	−0.24
$HoFe_2$[a]	3.6	−1.1	7	16	5.90	−0.19
$TbFe_2$[b]	4.5	−0.42	295			
$DyFe_2$[b]	4.2	−0.25	295			
$HoFe_2$[b]	4.1	−0.18	295			
$ErFe_2$[b]	4.0	−0.08	295			

[a]Lee (Ref. 14).
[b]Katayama and Hasegawa (Ref. 2).

$CeFe_2$ taken at 10 K and 10 kOe. Saturation is reached at 10 kOe (see inset), whereas the magnetic moment was observed to saturate at 6 kOe, even if the field is applied perpendicular to the easy axis. The shape of the Kerr spectrum is very similar to that of single-crystal $GdFe_2$.[14,42] However, the Kerr rotation is negative over the entire energy range. A local minimum appears in the Kerr rotation at 2 eV and a minimum Kerr rotation of −0.8° is found at 4.2 eV. This compares with the rotation measured for $HoFe_2$, despite the much smaller magnetic moment in $CeFe_2$. In Table I we summarize earlier experimental results and compare them to our data. First we note that there is no obvious systematic variation in the position of maximum Kerr effect $E_{\max}$ in Lee's data.[14] The largest Kerr rotation is found in $HoFe_2$ and the smallest for $GdFe_2$. If the Kerr effect were simply proportional to the net spin polarization (or magnetization), as derived from a simple model for the off-diagonal conductivity, we would extrapolate a Kerr rotation of less than −0.5° for $HoFe_2$. This indicates that there are other important factors which determine the off-diagonal optical conductivity in these compounds. Misemer[57] presented a systematic study of the size of magneto-optic effects and their dependence on spin-orbit splitting and exchange interaction. It was found that the off-diagonal conductivity is proportional to the spin-orbit interaction but shows no simple relationship with the magnetization. This is supported by the specific Kerr rotation, which is also shown in Table I. We define the specific Kerr rotation as the maximum observed Kerr rotation per magnetic moment. This indicates that $CeFe_2$ is the most *effective* material showing a Kerr rotation of $-0.29°/\mu_B$, which is similar to the value for $TbFe_2$. It becomes evident from the scattering of these values that there is no clear scheme that would allow us to predict the size of the Kerr rotation based on the sample magnetization. As pointed out by Misemer,[57] the Kerr effect is also proportional to the spin-orbit splitting. This is confirmed by $GdFe_2$, $TbFe_2$, and $HoFe_2$ in order of increasing spin-orbit interaction and Kerr rotation. However, YFe_2 and $CeFe_2$ do not fit in this scheme.

In order to compare our experimental results with LDA calculations we determined the optical conductivity from the optical constants (Fig. 4) and the Kerr parameters (Fig. 5). We show in the upper panel of Fig. 6 the experimental σ_{1xx} together with the conductivity calculated from the band structure. The calculated conductivity is reduced by a factor of 3. It was observed earlier that the magnitude of the optical conductivity is often overestimated by the calculation, which predicts values that are larger by a factor of 1.6 to 3.[58,42] Ellipsometry as well as MOKE is surface sensitive with typical penetration depths of 50–100 Å . The measured conductivities frequently fall below calculated values due to rough or contaminated surfaces. We would like to stress the structure of the spectra rather than the magnitude. A self-energy correction with $\lambda = -0.1$ and a lifetime broadening of 0.5 eV were used for the theoretical spectrum.[59,60] The shoulder at 2.8 eV is well reproduced and a broad shoulder around 4.8 eV can be identified in the calculated spectrum. The off-diagonal conductivity (lower panel) agrees well with the calculated σ_{2xy}. The absorption falls off monotonically reaching a minimum at 3.4 eV. There is a shoulder at 2 eV which is also seen in the calculated spectrum. The spectrum is similar to that for $LuFe_2$ measured by Lee *et al.*[14,42] Absorption then increases again towards higher energy and a relative maximum is found at 4.5 eV.

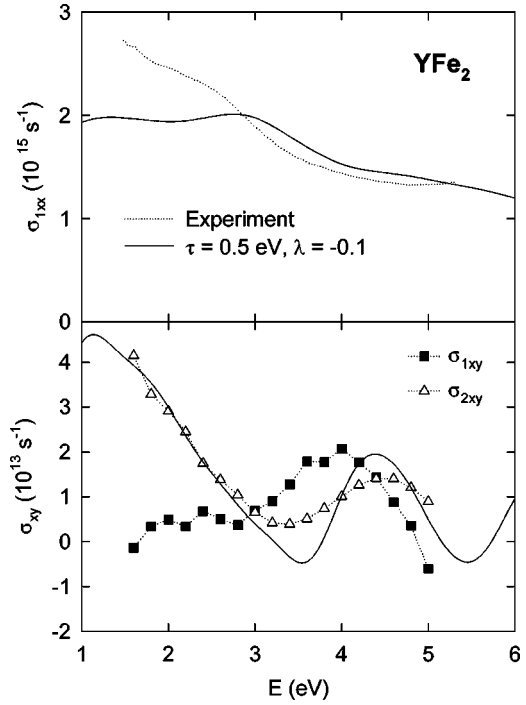

FIG. 6. Upper panel shows the absorptive component of the diagonal part of the conductivity of YFe_2. The solid line indicates the result obtained from our calculation including a self-energy correction with $\lambda = -0.1$ and a lifetime broadening of 0.5 eV. The lower panel shows the off-diagonal optical conductivity. The solid line represents the theoretical result. The magnitude of the calculated σ_{1xx} and σ_{2xy} has been reduced by a factor of 3.

A comparison of the absorptive part of the off-diagonal conductivity of YFe_2 with that of $CeFe_2$ is shown in Fig. 7. The upper panel shows σ_{xy} for $CeFe_2$. The spectrum is similar to that of YFe_2 in Fig. 6. Even the shoulder at 2 eV is present in this compound. The contribution of free carriers is proportional to ω^{-1}. To remove the effects of free carriers

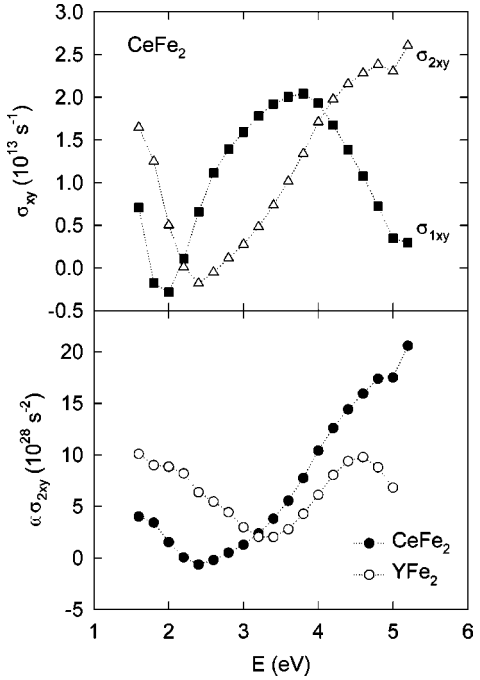

FIG. 7. The off-diagonal optical conductivity of $CeFe_2$ is shown in the upper panel. The lower part shows $\omega\sigma_{2xy}$ for YFe_2 and $CeFe_2$.

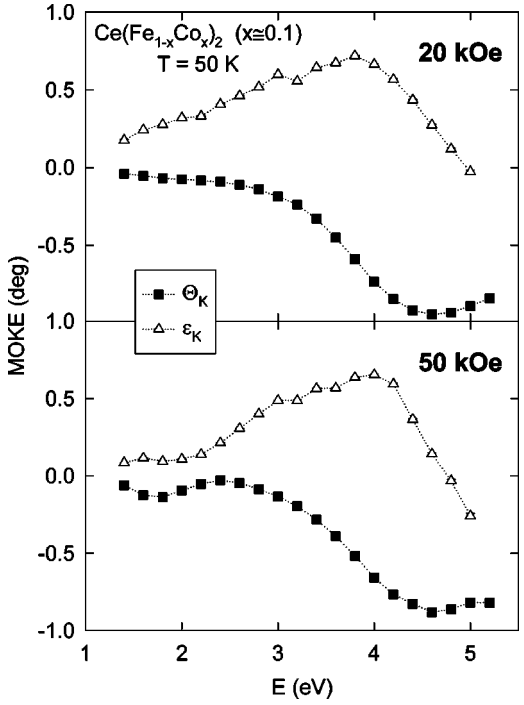

FIG. 8. Kerr rotation (Θ_K) and ellipticity (ϵ_K) for $Ce(Fe_{1-x}Co_x)_2$ ($x \simeq 0.1$) at 50 K.

we show $\omega\sigma_{2xy}$ in the lower panel of that figure. Also shown is the spectrum for YFe_2. This emphasizes the similar structures observed in both compounds. The amplitude of the transition at 4.5 eV is smaller and the minimum occurs at a higher energy in YFe_2 than in $CeFe_2$. Since these features are not found in spectra of RAl_2 (R=Ce,Pr) (Ref. 61) this implies that they can be ascribed to Fe. Contrary to the Kerr effect, which shows a structure around 2 eV in $CeFe_2$ but not in YFe_2, $\omega\sigma_{2xy}$ is very similar for the two compounds. This would lead to the conclusion that this part of the spectrum is either Fe related or due to transitions involving rare-earth d states, which are very similar in both compounds.

After describing the spectra for YFe_2 and $CeFe_2$ let us now turn to the most intriguing sample. At 50 K $Ce(Fe_{1-x}Co_x)_2$ ($x \simeq 0.1$) orders antiferromagnetically in zero field. It was shown that a metamagnetic transition to a state with long-range ferromagnetic order occurs at 30 kOe. In our experiment we apply a field parallel to [111], i.e., perpendicular to the easy axis in this compound, and the magnetization data in Fig. 3 do not necessarily represent the actual magnetization of the sample in our experiment. However, since the anisotropy is small, the net magnetization at 20 kOe will be very small. Figure 8 shows Kerr spectra taken at 50 K in fields of 20 and 50 kOe. Despite the small moment at 20 kOe we observed a large Kerr rotation that nearly reaches $-1°$. The broad maximum around 4.6 eV is the dominant feature of the spectrum and compares well with that found in $CeFe_2$. There is a very weak structure at 2 eV. At the same position we found a feature in $CeFe_2$. This indicates that the transition might still be present but is weaker due to different magnetic order. In a larger field (50 kOe) ferromagnetic order is induced and the shape of the Kerr rotation more closely resembles that of $CeFe_2$. The main difference compared to the data taken at lower field is the reappearance of the 2 eV structure. This was expected since in the ferromagnetic state $CeFe_2$ and $Ce(Fe_{1-x}Co_x)_2$ ($x \simeq 0.1$) should be similar. To emphasize the difference we compare the Kerr rotation at 20 and 50 kOe with that of $CeFe_2$ in Fig. 9. The minimum in Θ_K is shifted by 0.2 eV to higher energy with respect to $CeFe_2$ and the maximum rotation is increased by nearly 0.2°. Let us focus on the difference between the 20 and 50 kOe data. At 2 eV the Kerr rotation is larger in the ferromagnetic state whereas for $E > 2$ eV the Kerr rotation in the antiferromagnetic state is larger. In order to check this field dependence of the Kerr rotation we measured Kerr loops at different temperatures and energies (Fig. 10). Note that Kerr loops were taken on a different sample. Thus the reduced magnitude of the Kerr rotation indicates a thicker oxide layer on this specimen. The center panel shows the same experimental conditions dis-

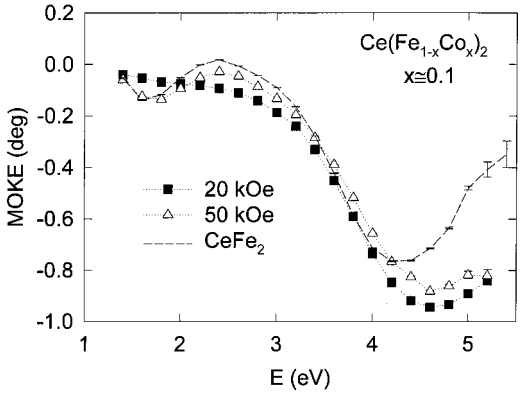

FIG. 9. Kerr rotation for $Ce(Fe_{1-x}Co_x)_2$ ($x \simeq 0.1$) at 50 K in the antiferromagnetic (20 kOe) and ferromagnetic (50 kOe) state. We also show the Kerr rotation of $CeFe_2$ in the saturated regime.

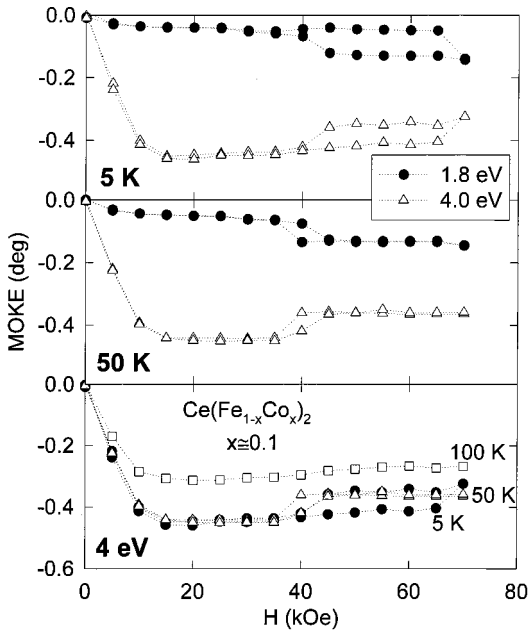

FIG. 10. Field and temperature dependence of the Kerr rotation of $Ce(Fe_{1-x}Co_x)_2$ ($x \simeq 0.1$). The upper two panels show the Kerr rotation at 1.8 and 4 eV taken at 5 and 50 K, respectively. The lower panel shows the Kerr rotation at 4 eV at 5, 50, and 100 K.

cussed above. We measured the Kerr rotation at 50 K at 1.8 and 4.0 eV. At 1.8 eV Θ_K increases to about $-0.05°$ and saturates before ferromagnetic order is induced at 40 kOe and Θ_K increases to $-0.14°$. Θ_K saturates and remains constant up to 70 kOe. The situation is much more dramatic at 4 eV. Despite a small magnetic moment the Kerr rotation reaches $-0.45°$ and shows the same field-induced transition at 40 kOe. But this time the transition occurs to a smaller Kerr rotation, i.e., the magnitude of the Kerr rotation is reduced for an increased magnetization. This is very unusual and we performed measurements on another sample which confirmed our observation. Due to instrumental limitations ($H_{\max}$ for the magnetometer is 55 kOe) it was not possible to see a phase transition at 5 K in the magnetization data. Our optical cryostat allows fields up to 70 kOe and we actually found the same transition to occur between 65 and 70 kOe at 5 K. This is shown in the upper panel of Fig. 10. Θ_K is similar to the loops taken at 50 K, the only difference being an increased hysteresis at lower temperature. The same transition was found at 68 kOe in a polycrystalline sample of similar composition.[29] The metamagnetic transition is observed at even higher field but data were taken at a lower temperature, which increases the critical field. What makes this material so interesting is the large Kerr rotation at 4 eV in a region of very low magnetization. In the lower panel of Fig. 10 we compare data taken at 4 eV for three different temperatures. The magnitudes of the Kerr rotation observed at 5 and 50 K are in good agreement. For both temperatures Θ_K has the same value in the ferromagnetic as well as in the antiferromagnetic phase. The only difference is a stronger hysteresis due to a higher critical field at lower temperature. At 100 K the sample is in the ferromagnetic state and Θ_K saturates at 10 kOe. The magnitude is reduced compared to that in the field induced ferromagnetic phase. This is due to a reduced magnetization (see Fig. 3).

VI. CONCLUSIONS

Comparing the shape of our MO spectra in Fig. 5 with those of heavier RFe_2 compounds[2] we find that all spectra show a broad minimum in the Kerr rotation between 3.5 and 5 eV. The measurements by Katayama and Hasegawa[2] show a decrease of the magnitude of Θ_K with increasing atomic number of the rare earth. Furthermore, the minimum shifts to lower energy in compounds with heavier rare earths. However, the structure of the spectra changes very little for different compounds. We therefore ascribe this part of the spectrum to Fe-*d* derived transitions. This structure is absent in the spectra of RAl_2 (Ref. 61) which supports our conclusion. The low-energy absorption spectra of RAl_2 and RFe_2 are very similar. Rare-earth *p* and *d* states do not change significantly as the *f* shell is filled, and we observe similar structures in Θ_K in the heavy RFe_2.[2,14] We assign the structure around 2 eV to rare-earth derived transitions involving *d* states. As expected, this absorption is also found in the σ_{2xy} spectrum of YFe_2. Rare-earth *f* states polarize the *d* states which yields an appreciable magneto-optical signal in RM_2 compounds. As found for RAl_2, the *d* moment itself can be rather small.[61]

In the case of RAl_2 Θ_K is proportional to the sample magnetization. This is due to the simple magnetic structure of those compounds. Only the rare earth carries a moment (which is more than 80% $4f$) and through intra-atomic coupling the spin polarization of the $5d$ states is proportional to the spin magnetization. For RFe_2 the situation is more complicated since the rare earth, as well as the Fe, carries a moment. In Fig. 5 the insets show the saturation behavior for YFe_2 and $CeFe_2$. There is a nearly linear increase in Θ_K and saturation sets in at 10 kOe. This corresponds to a ferrimagnetic alignment of the Fe and rare-earth magnetic moment along [111].

From magnetization and Kerr angle versus field data for antiferromagnetic $Ce(Fe_{1-x}Co_x)_2(x \simeq 0.1)$ it emerges that there is a fairly large MO response despite a quite minute net magnetic moment at 50 K and 20 kOe. Magnetization increases linearly until *H* approaches the critical field. It differs from the Kerr rotation which saturates at an external field of 20 kOe. This could possibly indicate saturation of a magnetic sublevel which contributes to this absorption. According to neutron scattering the Ce-$5d$ and $4f$ moment is small ($<0.04\mu_B$) and cannot be seen in our magnetization measurements. Another possible scenario is the formation of a magnetic surface layer which saturates at a lower field than the bulk of the sample. Magnetic x-ray scattering at grazing incidence could help to determine if there is such a layer and if its magnetic behavior differs from that of the bulk of the sample. Above the metamagnetic transition the Fe moments align ferromagnetically which leads to a steep increase in the magnetization. However, the change in the magneto-optic signal is an order of magnitude smaller. It appears that we are able to detect a much smaller magnetic moment using the Kerr effect, which selectively probes particular electronic states. The exact origin of the MO spectra at 1.8 and 4 eV has not been determined unambiguously. One should keep in mind that there are other effects that we have not considered

in the previous analysis. There is a structural distortion at T_N which is reversed as the field is increased and ferromagnetic order on the Fe sublattice is restored. This distortion can lead to splitting of bands which will change the spectrum. Furthermore the Brillouin zone in the antiferromagnetic regime is smaller than for the ferromagnetic structure, i.e., the chemical unit cell is doubled due to antiferromagnetic spins on the Fe ions in consecutive (111) planes. This may lead to band folding and opening of gaps which are not present in the ferromagnetic BS.

ACKNOWLEDGMENTS

Ames Laboratory is operated for the U.S. Department of Energy by Iowa State University under Contract No. W-7405-Eng-82. This work was supported by the Director of Energy Research, Office of Basic Energy Science.

[1] K. H. J. Buschow, Rep. Prog. Phys. **40**, 1179 (1977).
[2] T. Katayama and K. Hasegawa, in *Rapidly Quenched Metals*, edited by T. Masumoto and K. Suzuki (Japan Institute of Metals, Sendai, 1982), Vol. 4, p. 915.
[3] S. B. Roy and B. R. Coles, J. Phys.: Condens. Matter **1**, 419 (1989).
[4] S. B. Roy and B. R. Coles, Phys. Rev. B **39**, 9360 (1990).
[5] S. J. Kennedy and B. R. Coles, J. Phys.: Condens. Matter **2**, 1213 (1990).
[6] C. S. Garde, J. Ray, and G. Chandra, Phys. Rev. B **42**, 8643 (1990).
[7] L. Paolasini, P. Dervenagas, P. Vulliet, J.-P. Sanchez, G. H. Lander, A. Hiess, A. Panchula, and P. Canfield, Phys. Rev. B **58**, 12 117 (1998).
[8] M. Croft, R. Neifield, B. Qi, G. Liang, I. Perez, S. Gunapala, F. Lu, S. A. Shaheen, E. G. Spencer, N. Stoffel, and M. den Boer, in *5th International Conference on Valence Fluctuations*, edited by S. K. Malik and L. C. Gupta (Plenum Press, New York, 1987), Vol. 1, p. 217.
[9] S. J. Kennedy, P. J. Brown, and B. R. Coles, J. Phys.: Condens. Matter **5**, 5169 (1993).
[10] B. Johansson, O. Eriksson, L. Nordström, L. Severin, and M. S. S. Brooks, Physica B **172**, 101 (1991).
[11] M. S. S. Brooks and B. Johansson, in *Handbook of Magnetic Materials*, edited by K. H. J. Buschow (North-Holland, Amsterdam, 1993), Vol. 7, p. 139.
[12] Z. Fisk and J. P. Remeika, in *Handbook on the Physics and Chemistry of Rare Earths*, edited by K. A. Gschneidner, Jr. and L. Eyring (Elsevier Science Publishers, London, 1989), Vol. 12, p. 53.
[13] P. C. Canfield and Z. Fisk, Philos. Mag. B **65**, 1117 (1992).
[14] S. J. Lee, R. J. Lange, P. C. Canfield, B. N. Harmon, and D. W. Lynch (unpublished).
[15] K. H. J. Buschow and R. P. van Stapele, J. Appl. Phys. **41**, 4066 (1970).
[16] G. L. Olcese, Boll. Sci. Fac. Chim. Ind. Bologna **24**, 165 (1966).
[17] K. Ideka and K. A. Gschneidner, Jr., Phys. Rev. Lett. **45**, 1341 (1980).
[18] C. Ritter, J. Phys.: Condens. Matter **1**, 2765 (1989).
[19] A. Arrott, Phys. Rev. **108**, 1394 (1957).
[20] H. G. Farrell and W. E. Wallace, J. Chem. Phys. **40**, 1167 (1964).
[21] C. Giorgetti, S. Pizzini, E. Dartyge, A. Fontaine, F. Baudelet, C. Brouder, Ph. Bauer, G. Krill, S. Miraglia, D. Fruchart, and J. P. Kappler, Phys. Rev. B **48**, 12 732 (1993).
[22] J. Ph. Schillé, F. Bertran, M. Finazzi, Ch. Brouder, J. P. Kappler, and G. Krill, Phys. Rev. B **50**, 2985 (1994).
[23] A. Delobbe, A. M. Dias, M. Finazzi, L. Stichauer, J. P. Kappler, and G. Krill, Europhys. Lett. **43**, 320 (1998).
[24] M. J. Cooper, P. K. Lawson, M. A. G. Dixon, E. Zukowski, D. N. Timms, F. Itoh, H. Sakurai, H. Kawata, Y. Tanaka, and M. Ito, Phys. Rev. B **54**, 4068 (1996).
[25] V. S. Pokatilov, J. Magn. Magn. Mater. **189**, 189 (1998).
[26] S. J. Kennedy, A. P. Murani, J. K. Cockroft, and B. R. Coles, J. Phys.: Condens. Matter **1**, 629 (1989).
[27] S. J. Kennedy, A. P. Murani, B. R. Coles, and O. Moze, J. Phys. F **18**, 2499 (1988).
[28] H. Wada, M. Nishigori, and M. Shiga, J. Phys.: Condens. Matter **3**, 2083 (1991).
[29] H. Wada, M. Nishigori, and M. Shiga, J. Phys. Soc. Jpn. **62**, 1337 (1993).
[30] H. Wada, T. Harada, and M. Shiga, J. Phys.: Condens. Matter **9**, 9347 (1997).
[31] N. Ali and X. Zhang, Int. J. Mod. Phys. B **7**, 822 (1993).
[32] X. Zhang and N. Ali, J. Alloys Compd. **207/208**, 300 (1994).
[33] O. K. Andersen, O. Jepsen, and D. Glötzel, in *Highlights of Condensed-Matter Theory*, edited by F. Bassani, F. Fumi, and M. P. Tosi (North-Holland, New York, 1985), Vol. 1, p. 59.
[34] U. von Barth and L. Hedin, J. Phys. C **5**, 1629 (1972).
[35] X. Wang, V. P. Antropov, and B. N. Harmon, IEEE Trans. Magn. **30**, 4458 (1994).
[36] H. Yamada, J. Inoue, K. Terao, S. Kanda, and M. Shimizu, J. Phys. F **14**, 1943 (1984).
[37] P. Mohn and K. Schwarz, Physica B **130**, 26 (1985).
[38] O. Eriksson, L. Nordström, M. S. S. Brooks, and B. Johansson, Phys. Rev. Lett. **60**, 2523 (1988).
[39] O. Eriksson, B. Johansson, M. S. S. Brooks, and H. L. Skriver, Phys. Rev. B **40**, 9519 (1989).
[40] O. Eriksson, L. Nordström, A. Pohl, L. Severin, A. M. Boring, and B. Johansson, Phys. Rev. B **41**, 11 807 (1990).
[41] J. Y. Rhee, J. Phys.: Condens. Matter **10**, 4307 (1998).
[42] S. J. Lee, R. J. Lange, S. Hong, S. Zollner, P. C. Canfield, A. F. Panchula, B. N. Harmon, and D. W. Lynch, Thin Solid Films **313-314**, 223 (1998).
[43] R. M. A. Azzam and N. M. Bashara, *Ellipsometry and Polarized Light* (North-Holland, Amsterdam, 1977).
[44] D. E. Aspnes and A. A. Studna, Appl. Opt. **14**, 220 (1975).
[45] R. W. Collins, Rev. Sci. Instrum. **61**, 2029 (1990).
[46] J. L. Erskine and E. A. Stern, Phys. Rev. B **12**, 5016 (1975).
[47] J. Schoenes, in *Materials Science and Technology*, edited by R. W. Cahn, P. Haasen, and E. J. Kramer (VCH, Weinheim, 1991), Vol. 3A, p. 147.
[48] S. N. Jasperson and S. E. Schnatterly, Rev. Sci. Instrum. **40**, 761 (1969).
[49] L. F. Mollenauer, D. Downie, H. Engstrom, and W. B. Grant, Appl. Opt. **8**, 661 (1969).
[50] J. C. Kemp, J. Opt. Soc. Am. **59**, 950 (1969).
[51] G. A. Osborne, J. C. Cheng, and P. J. Stephens, Rev. Sci. Instrum. **44**, 10 (1973).

[52] K. W. Hipps and G. A. Crosby, J. Phys. Chem. **83**, 555 (1979).
[53] K. Sato, Jpn. J. Appl. Phys. **20**, 2403 (1981).
[54] K. Sato, H. Hongu, H. Ikekame, Y. Tosaka, M. Watanabe, K. Takanashi, and H. Fujimori, Jpn. J. Appl. Phys., Part 1 **32**, 989 (1993).
[55] W. S. Kim, M. Aderholz, and W. Kleemann, Meas. Sci. Technol. **4**, 1275 (1993).
[56] Sh. M. Sharipov, K. M. Mukimov, L. A. Ernazarova, A. V. Andreyev, and N. V. Kudrevatykii, Phys. Met. Metallogr. **69**, 50 (1990).
[57] D. K. Misemer, J. Magn. Magn. Mater. **72**, 267 (1988).
[58] R. J. Lange, S. J. Lee, D. W. Lynch, P. C. Canfield, B. N. Harmon, and S. Zollner, Phys. Rev. B **58**, 351 (1998).
[59] J. F. Janak, A. R. Williams, and V. L. Moruzzi, Phys. Rev. B **11**, 1522 (1975).
[60] J. E. Müller, O. Jepsen, and J. W. Wilkins, Solid State Commun. **42**, 365 (1982).
[61] R. J. Lange, I. R. Fisher, P. C. Canfield, and D. W. Lynch (unpublished).
[62] R. J. Lange, Ph.D. thesis, Iowa State University, 1999.